Journal of Pharmaceutical & Biomedical Analysis
Vol. 9, No. 9, pp. 679–684, 1991
Printed in Great Britain

0731–7085/91 $3.00 + 0.00
Pergamon Press plc

Kinetic determination of aspartate aminotransferase in human serum with a flow-injection/multidetection system

J.M. FERNÁNDEZ-ROMERO* and M.D. LUQUE DE CASTRO

Department of Analytical Chemistry, Faculty of Sciences, University of Córdoba, 14004, Córdoba, Spain

Abstract: Photometric–kinetic methods for the determination of activity of aspartate aminotransferase are proposed. The flow-injection manifold used for this purpose includes a selecting valve which allows the sample to be trapped in a closed circuit where a solid reactor housing an auxiliary enzyme and a conventional single detector allows a multipeak recording to be obtained for each sample. This record represents a typical kinetic curve from which much information can be obtained to develop fixed-time and reaction-rate methods for the determination of the analyte based on its catalytic action on the L-aspartic acid–2 oxoglutarate system. The linear range is found to be between 1 and 500 U l^{-1}, with relative standard deviation less than 1%. The utility of the methods is illustrated by the determination of the analyte in human serum from healthy and sick individuals.

Keywords: *Enzymatic activity; aspartate aminotransferase; kinetic; immobilization; multidetection; photometry; serum; FIA.*

Introduction

The enzyme aspartate aminotransferase (AST/GOT) (L-aspartic 2-oxoglutarate aminotransferase, EC 2.6.1.1.) catalyses the reversible transfer of the amino group in aspartic acid to 2-oxoglutarate to yield oxaloacetate and L-glutamate according to:

$$\text{L-aspartic acid} + \text{2-oxoglutarate} \overset{\text{AST}}{\rightleftharpoons} \text{oxaloacetate} + \text{L-glutamate}.$$

This enzyme is distributed in different body tissues and its concentration in human serum is found to increase as a result of various hepatic and cardiac disorders. Thus, the determination of AST activity is a potential aid to the diagnosis of these types of disorder.

The determination of AST activity is usually based upon the indirect measurement of the oxaloacetate produced in the reaction catalysed by the enzyme. Several kinetic–photometric methods for the determination of the activity of this enzyme have been developed according to the recommendations of the American Chemical Association for Clinical Chemistry [1] and the Sociedad Española de Química Clínica [2], by using an open–closed flow-injection configuration [3–5]. In the present work a coupled indicator reaction to the transamination reaction in which the oxaloacetato is reduced to malate with the aid of the coenzyme NAD^+ in its reduced form and in the presence of malate dehydrogenase (MDH) has been developed. The reaction is monitored through the absorbance decrease at 340 nm owing to the consumption of NADH (indicator reagent).

Experimental

Reagents

Stock solutions: 100 mM tris(hydroxymethyl) amino methane (TRIS) buffer, adjusted to pH 7.5 with 1 M HNO_3; 100 mM NADH (Sigma, St Louis, MO, USA) prepared in 30% ethylene glycol–water; 100 U of glutamic–oxalacetic transaminase (Sigma) prepared in TRIS buffer; 0.1 M 2-oxoglutarate (Sigma); 1 M L-aspartic acid (Sigma) also prepared in TRIS buffer. Controlled-pore glass (CPG 120–200 mesh, Electronucleonics, Fairfield, USA) was used to immobilize the auxiliary enzyme as described by Massom and Townshend [6].

* Author to whom correspondence should be addressed.

Equipment

A Pye-Unicam Model SP-500 single-beam spectrophotometer equipped with a Hellma 178.12 QS flow-cell (address) was connected to a Radiometer recorder (address). A four-channel Gilson Minipuls-2 peristaltic pump with rate selector, two Rheodyne Model 5041 injection valves (one modified to act as a selecting valve) (address), a Tecator TM-III chemifold and a Selecta 382-S thermostat were used (address). A Leo PC system equipped with a DAS–8PGA interface (Metrabyte, address) was used to capture the absorbance-time data and the absorbance values at the maxima and minima.

FIA manifold

The configuration used (Fig. 1) consists of a peristaltic pump (P_1) which propels a reagent stream through the different channels of the open system, an injection system (IS), a selecting valve (SV) switching of which enables the circuit to be opened and closed, an immobilized enzyme reactor (IMER) containing the auxiliary enzyme (MDH) immobilized on controlled-pore glass (PGC), a flow-cell located in the photometric detector and another peristaltic pump (P_2) that can be a channel of P_1, which established the flow in the closed circuit. All inner diameter of tubing was 0.5 mm, except for the IMER (1.0 mm).

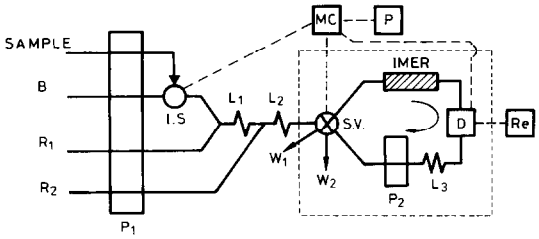

Figure 1
Open–closed configuration for determination of AST/GOT. R = reagent, P = peristaltic pump, IS = injection system, L = reactor, W = waste, SV = selecting valve, IMER = immobilized enzyme reactor, D = detector, Re = recorder, MC = microcomputer, and P = printer.

The sample is injected into a stream of TRIS buffer (R_1) and successively merges with the two substrates of the main reaction: 2-oxoglutarate in TRIS buffer (R_2) and L-aspartic acid and NADH also in TRIS buffer (R_3), the mixing process and the transamination reaction taking place along reactor L_1 and L_2. The switching of the selecting valve at a preset time from injection allows the reacting plug to be trapped in the closed circuit; this plug passes through the enzymatic reactor (IMER), starting the indicator reaction, which is monitored as the plug passes through the spectrophotometer flow-cell (D). The iterative passage of the plug through the IMER and the detector also allows the iterative development of the indicator reaction and its detection. The data generated are collected by the computer (PC) for subsequent treatment and results are presented by means of the printer (P). Optionally, multipeak signals can be obtained by the recorder.

Procedure

The serum sample is suitably diluted with TRIS buffer before being injected into the FIA system, which operated as described above. The collected data are treated with a simple program and the value of the selected parameter is compared with the calibration curve.

Results and Discussion

Recordings

The iterative passage of the sample plug through the IMER and the detector provides a multipeak recording in which successive decreases in the absorbance correspond to increasing extents of reaction development.

Data acquisition and treatment

The net data corresponding to the analyte activity result from the treatment of the data provided by three multipeak recordings:

(a) overall sample signal (S_s) obtained on injecting the sample;
(b) sample blank (S_b) obtained by replacing the injected sample value with the buffer in which the sample is diluted;
(c) reagent blank (S_r) obtained by injecting the sample into the system, but previously removing one of the substrates (2-oxoglutarate), which does not absorb at 340 nm.

The net signal is obtained by means of the expression:

$$S_n = S_s - (S_b + S_r).$$

A computer program allows the S_b and S_r recordings to be collected and stored to obtain the net recording for each sample, from which several methods can be implemented depend-

ing on the measurement parameter used, namely:

(a) fixed-time measurements, based on the signal corresponding to the maxima (S_{s1}, S_{s2}, . . . S_{sn}), or minima (S'_{s1}, S'_{s2}, . . . S'_{sn}) of the multipeak recording;
(b) reaction-time measurements, based on the absorbance decrease between two successive maxima or minima, divided by the interval between their appearances ($v_n = (S_{s(n+1)} - S_{sn})/(t_{n+1} - t_n)$), or ($v'_n = (S'_{s(n+1)} - S'_{sn})/(t_{n+1} - t'_n)$);
(c) methods for expanding sensitivity [7], based on the sum of several signals (ΣS_{si}, $\Sigma S'_{si}$, $\Sigma v'_i$ or Σv_i).

Optimization of the system

A study of the different variables that influence the system was performed. They were grouped into chemical, FIA and physical. Table 1 shows the range over which each was studied and its optimum value.

Chemical variables. A buffer of tris (hydroxymethyl)aminomethane was used according to literature recommendations; its pH was adjusted between 6.0 and 8.5 with HNO_3 or NaOH and all solutions and samples were prepared using it. The net signal was found to increase with the pH up to 7.50, above which it decreased because the auxiliary enzyme and the analyte itself became unstable. A concentration of 0.1 M of this buffer provided the best signals.

An increase in the concentration of L-aspartic acid increased the signal up to 200 mM, above which the signal remained almost constant. The other substrate of the main reaction (2-oxoglutarate) showed a similar behaviour up to a concentration of 6 mM.

The optimum concentration of the indicator reagent, NADH, was that giving rise to a high baseline without saturating the detector capacity, so as to ensure that the decrease range was as wide as possible. A concentration of 1.0 mM of NADH provided a baseline close to 1.000 units (AU), which was considered to be the best value.

The optimum length of the enzymatic reactor was 5 cm, above which the recording remained constant at any fixed analyte concentration between 1 and 600 U l^{-1}.

Increased temperatures had a positive effect on the reaction rate up to 40°C; above this value, the signals decreased, possibly because of the instability of the reagents and/or denaturation of the analyte and auxiliary enzyme.

FIA variables. The injected volume was a key variable as it conditioned the sample volume/closed circuit volume ratio and hence the extent of dilution the enzyme–analyte underwent during multidetection. Thus, this variable was optimized together with the length of reactor L_3 to ensure the optimum ratio, namely 5:8 v_i:L_3.

The flow-rate in the closed circuit is another important variable of this type of system as the flow-rate influences the duration of the iterative detection process, which in turn depends on the interval elapsed until complete homogenization of the sample and reagents in the closed circuit is achieved. A flow-rate of 0.97 ml min^{-1} provided the best net signal.

The lengths of L_1 and L_2 determined the extent of the development of the main reaction before the derivatizing reaction was started;

Table 1
Range studied and optimum values of variables

Variable		Range studied	Optimum value
Flow rate (ml min^{-1})		0.47–1.80	0.97
Injection volume (μl)		60–600	500
Reactor length (cm)	L_1	—	15
	L_2	50–250	200
	L_3	25–250	100
Buffer (M)		TRIS–HNO_3	0.1
pH		6.00–8.50	7.50
[NADH] (mM)		—	1.0
[Aspartic acid] (mM)		25–400	200
[2-oxoglutarate] (mM)		0.5–20	6.0
Length of IMER (cm)		2.0–10.0	5.0
Temperature (°C)		20–45	40
Switching time (s)		60–180	75

thus, it can be regarded as an induction period of the auxiliary reaction. The optimum values of these reactor lengths are listed in Table 1.

Switching the selecting valve changed the open into a closed configuration. The interval between injection and switching resulted in the complete partial or nil trapping of the reactant plug inside the closed circuit; the optimum time was 75 s.

Calculation of the Michaelis–Menten constants (reference). The Michaelis constants for each of the substrates taking part in the main reaction (catalysis from AST/GOT) were calculated by applying Lineweaver–Burk plots (reference). The values of these were K_M(2 oxoglutarate, mM) = 3.804, and K_M(aspartic acid, mM) = 317.580. Calculations were made taking no account of the inhibitory effects of the rest of the substrates on each substrate studied [8].

Calibration curves and reproducibility

With the optimum values of the variables (Table 1) a series of nine standards with activities between 1 and 600 U l^{-1} were injected in triplicate. The treatment of the data obtained provided two fan-shaped sets of calibration curves corresponding to fixed-time and reaction-rate measurements. The signals always correspond to net values.

Table 2 summarizes the features of these curves (intercept, slope, regression coefficient, linear range and reproducibility) for the method based on fixed-time measurements (maxima, minima and sum of several signals). The curve obtained from the first minimum (slope 7.210×10^{-4}) is the less sensitive whilst that obtained from the sum of the first three maxima (slope 6.625×10^{-3}) displays the best sensitivity for fixed-time measurements. Table 2 also summarizes the features of the calibration curves obtained from parameters based on reaction-rate measurements. Similarly, an increase in sensitivity can be observed in the slope of the calibration curves from v_1 to $\sum_1^3 v_i$. The linear regression coefficient was higher than 0.99 in all instances.

The linear determination ranges were between 1 and 200, and 1 and 500 U l^{-1}.

The reproducibility of the methods, expressed as the RSD, was studied on 11 samples of AST/GOT with an activity of 30 U l^{-1}, and was found to range between 0.29 and 1.05 (see Table 2).

The sampling frequency depended on the measurement parameter used and ranges between 65 h^{-1} (measurement of the first maximum) and 20 h^{-1} (measurement of the third minimum).

Application of the proposed methods to the determination of AST/GOT in human serum

As a preliminary step the activity of the analyte in 10 samples from healthy and sick individuals was determined by using the IFCC standard method [1]; then, the proposed methods were applied to the determination of AST/GOT in these samples in two ways, namely:

(a) determination of the analyte in each sample. Table 3 summarizes the most representative types of measurements;
(b) study of the recovery afforded by the proposed method after addition of 25 and

Table 2
Equations and features of the calibration graphs based on fixed-time (A) and reaction-rate (v) measurements

Measured parameter	Equation	r^2	Range (U l^{-1})	RSD*	Sampling frequency (h^{-1})
S'_{n1}	$S'_{n1} = -0.006 + 7.210 \times 10^{-4}$[AST/GOT]	0.999	1–500	0.96	36
S_{n1}	$S_{n1} = 0.013 + 1.012 \times 10^{-3}$[AST/GOT]	0.996	1–500	0.29	65
S'_{n3}	$S'_{n3} = 0.112 + 2.336 \times 10^{-3}$[AST/GOT]	0.998	1–200	0.76	20
S_{n3}	$S_{n3} = 0.150 + 3.464 \times 10^{-3}$[AST/GOT]	0.993	1–200	1.05	25
$\sum_1^3 S_{ni}$	$\sum_1^3 S_{ni} = 0.220 + 6.625 \times 10^{-3}$[AST/GOT]	0.997	1–200	0.68	25
v_1	$v_1 = 4.574 \times 10^{-5} + 1.748 \times 10^{-6}$[AST/GOT]	0.999	1–200	0.69	65
v'_1	$v'_1 = -8.361 \times 10^{-5} + 9.244 \times 10^{-6}$[AST/GOT]	0.999	1–500	0.86	36
v_3	$v_3 = 0.715 \times 10^{-3} + 1.653 \times 10^{-5}$[AST/GOT]	0.993	1–200	1.05	25
$\sum_1^3 v_i$	$\sum_1^3 v_i = 1.044 \times 10^{-3} + 3.160 \times 10^{-5}$[AST/GOT]	0.997	1–200	0.49	25

*Concentration of AST/GOT = 50 U l^{-1}.

Table 3
Comparison of the results obtained by different measurements

	AST/GOT found ($U\ l^{-1}$)									
	Proposed method									
Sample	S'_{n1}	S_{n1}	S'_{n3}	S_{n3}	$\sum_1^3 S_{ni}$	v_1	v'_1	v_3	$\sum_1^3 v_i$	Standard method
1	34.99	34.93	35.00	34.90	34.97	34.99	35.00	35.00	34.90	35.00
2	16.00	16.15	15.74	16.05	15.95	15.38	15.99	16.09	16.01	16.00
3	27.95	28.01	28.15	27.88	28.03	27.79	27.99	27.91	28.08	28.00
4	6.79	7.06	6.75	6.81	6.75	6.69	6.90	6.88	6.84	6.80
5	7.90	8.25	8.04	7.97	7.95	8.05	7.90	8.03	8.04	8.00
6	119.90	119.90	119.97	119.97	119.95	119.43	119.90	119.81	119.94	120.00
7	38.17	37.89	37.57	37.99	37.99	37.90	38.17	37.99	38.76	38.00
8	18.75	19.10	18.73	18.93	19.00	19.00	18.99	18.96	19.06	19.00
9	8.90	8.55	8.46	8.55	8.60	8.62	8.50	8.60	8.62	8.60
10	32.62	33.00	32.86	33.08	32.99	32.98	32.49	33.09	32.90	33.00

Table 4
Recovery of AGT/GOT in serum samples

Sample	AST/GOT added; ($U\ l^{-1}$)	Recovery with different methods (%)								
		S'_{n1}	S_{n1}	S'_{n3}	S_{n3}	$\sum_1^3 S_{ni}$	v_1	v'_1	v_3	$\sum_1^3 v_i$
1	25	99	99	100	102	99	100	99	100	99
	50	96	100	99	100	100	101	98	101	100
2	25	100	100	102	98	99	103	100	98	102
	50	100	100	101	99	100	100	99	99	98
3	25	96	99	96	102	99	100	100	102	104
	50	100	98	99	99	99	103	100	99	100
4	25	97	98	102	98	99	101	100	98	100
	50	98	98	99	99	100	96	99	99	102
5	25	102	98	96	98	99	95	95	98	101
	50	100	98	99	100	100	98	96	100	104
6	25	98	98	100	97	99	99	100	98	96
	50	100	105	100	100	100	100	100	100	104
7	25	96	99	102	104	99	94	96	103	100
	50	99	99	103	100	100	100	99	100	97
8	25	100	98	102	98	98	99	97	101	96
	50	100	99	101	100	99	98	99	100	102
9	25	100	101	102	96	99	101	100	100	99
	50	98	100	101	100	100	102	100	102	97
10	25	105	97	94	98	100	97	106	99	99
	50	95	95	101	99	100	98	96	100	98
Average each method		99.0	99.0	100.0	99.4	99.4	99.3	99.0	99.9	99.9

50 $U\ l^{-1}$ of AST/GOT to each sample and suitable dilution to fit the concentration within the linear range of the calibration curves. The recoveries listed in Table 4 are excellent (between 94 and 105%, averaging 99.0–100.0%).

Final Remarks

The undeniable usefulness of flow injection analysis in the area of clinical chemistry has been shown once more with the proposed methods.

The use of an open–closed configuration as a means of accomplishing multi-detection with a conventional detector offers the possibility of carrying out measurements based on reaction rate in addition to those conventional fixed-time FIA measurements. Thus, the selectivity of the methods is dramatically improved by eliminating matrix effects from the sample. In addition, the sensitivity also can be enhanced by using the sum of the signals.

The use of a reactor packed with CPG onto which the auxiliary enzyme is immobilized, decreases the cost per analysis and simplifies

the configuration and the manipulation of reagents.

Acknowledgement — The Comisión Interministerial de Ciencia y Tecnologia (CICyT) is thanked for financial support (Grant no. PA86-0146).

References

[1] Approved recommendation (1985) on IFCC methods for the measurement of catalytic concentration of enzymes III. International Federation of Clinical Chemistry (1986), *J. Clin. Biochem.* **24**, 481–495 (1986).

[2] F.J. Gella, J. Arenas, R. Durbán, R. Moreno and M.C. Pastor, *Quím. Clín.* **5**, 247–251 (1986).

[3] A. Ríos, M.D. Luque de Castro and M. Valcárcel, *Analyt. Chem.* **57**, 1803–1809 (1985).

[4] A. Ríos, M.D. Luque de Castro and M. Valcárcel, *Analyt. Chim. Acta* **179**, 463–468 (1986).

[5] A. Ríos, M.D. Luque de Castro and M. Valcárcel, *J. Chem. Educ.* **63**, 552–553 (1986).

[6] M. Masoom and A. Townshend, *Analyt. Chim. Acta* **166**, 111–119 (1984).

[7] A. Ríos, F. Lázaro, M.D. Luque de Castro and M. Valcárcel, *Analyt. Chim. Acta* **199**, 15–27 (1987).

[8] H.U. Bergmeyer, P. Scheive and A.W. Wahlefeld, *Clin. Chem.* **24**, 58–73 (1978).

[*Received for review 30 May 1990; revised manuscript received 29 October 1990*]